



Protective Effect of N-Acetylcysteine Against Aluminum-Induced Kidney Tissue Damage in Rats

Sercan Kaya¹ · Tuba Yalçın¹ · Murat Boydak² · Hasan Hüseyin Dönmez²

Received: 21 March 2022 / Accepted: 29 April 2022 / Published online: 12 May 2022
© The Author(s), under exclusive licence to Springer Science+Business Media, LLC, part of Springer Nature 2022

Abstract

Aluminum (AL) is an important nephrotoxic agent with a high daily exposure rate and property of accumulation in tissues. This study aimed to investigate the potential protective efficacy of N-acetylcysteine (NAC) against AL exposure-induced nephrotoxicity in rats. Twenty-eight rats were randomly divided into 4 groups as control, N-acetylcysteine group (NC), AL, and AL + NC, with an equal number of rats in each group ($n = 7$). No application was made to the control group. A total of 150 mg/kg/day NAC was administered to the NC group and 30 mg/kg/day AL was administered to the AL group intraperitoneally (i.p.). The AL + NC group received 30 mg/kg/day AL and 150 mg/kg/day NAC i.p. Biochemical parameters in blood serum and histopathological changes in kidney tissue, oxidative stress parameters, spexin (SPX), and apoptotic protein levels were examined after 15 days. Histopathological changes, biochemical parameters, oxidative stress parameters, and apoptotic protein levels were significantly irregular in the AL group compared to the control group. Moreover, SPX levels increased in the AL group. However, NAC treatment regulated AL exposure-related changes in the AL + NC group. NAC treatment may have a prophylactic effect against nephrotoxicity due to AL exposure. SPX may play a role in AL-induced nephrotoxicity.

Keywords Aluminum · N-acetylcysteine · Spexin · Neuropeptide Q · Nephrotoxicity

Introduction

Aluminum (AL) is the third most abundant element in the earth's crust and is found in the environment, foodstuffs, and drinking water [1]. In addition, AL is a toxic metal and its exposure is gradually increasing [2]. Today, there is significant evidence that AL accumulation in tissues is associated with organ damage [3]. Most of AL is rapidly eliminated by the kidneys, possibly resulting in nephrotoxicity and renal failure [4]. It was reported that AL exposure adversely affects cellular structure and macromolecules that cause cytotoxicity, production of reactive oxygen species (ROS), mitochondrial dysfunction, inflammation, cell death, genetic damage, and carcinogenicity [5]. Furthermore, AL can deregulate ROS production and apoptosis by

stimulating the pro-oxidant properties of iron and copper, causing mitochondrial dysfunction and oxidative degradation of macromolecules, and the release of cytochrome C from mitochondria [6]. For this reason, neutralization and removal of free radicals can be considered as a candidate strategy to eliminate AL toxicity [7].

N-acetylcysteine (NAC) is a glutathione precursor with a thiol group that has antioxidant and anti-inflammatory effects [8]. NAC exhibits a strong antioxidant effect by increasing cellular glutathione (GSH) and consequently protects cells from lipid peroxidation [9]. It was also reported that the potent antioxidant effect of NAC makes it a potential control for disorders related to free radical damage [10].

Spexin (SPX), also known as neuropeptide Q, is a newly identified peptide, but information on its role in metabolism is limited. It is known that SPX is expressed in rat central nervous system and peripheral tissues such as the kidney, liver, lung, pancreas, stomach, skeletal muscle, and skin [11]. It was shown that SPX may play a role in the regulation of body weight, glucose metabolism, and secretion of key hormones responsible for the maintenance of homeostasis (insulin and leptin). Moreover, many studies reported an association between SPX levels and pathological conditions

✉ Sercan Kaya
sercan.kaya@batman.edu.tr

¹ Vocational Higher School of Healthcare Studies, Health Services Vocational School, Batman University, Batman, Turkey

² Department of Histology and Embryology, Faculty of Veterinary Medicine, Selçuk University, Konya, Turkey

such as obesity, type 2 diabetes, and metabolic syndrome [12–15].

There has always been a need for a therapeutic agent that can suppress the onset and progression of nephrotoxicity. This research was designed to determine the potential protective effect of NAC in regulating AL toxicity, oxidative stress, and apoptosis and its efficacy on the level of SPX in kidney tissue.

Materials and Methods

Animals and the Experimental Design

This study has been approved by the decision of the Dicle University Animal Testing Ethical Committee with the number 2021/26 and dated 09.09.2021. Optimal conditions for the care of the experimental animals were provided (12-h day/night, 22–25 °C temperature, 50% ± 10% humidity, add-libitum food, and water). Normal standard rat feed (in pellets) was obtained from the Dicle University Health Sciences Application and Research Center (DUHRC) (Table 1). Twenty-eight Sprague–Dawley male rats acquired from DUHRC (10 weeks old, 200–250-g weight) were randomly divided into 4 groups ($n = 7$): Control, NC, AL, and AL + NC. No application was made to the control group. For the NC group, 150 mg/kg dosed NAC was given intraperitoneally (i.p.) for 14 days every day. For the AL group, aluminum chloride (AlCl_3) (Sigma-Aldrich, Lot: BCBC6095V, 10 mg of AlCl_3 was dissolved in 1 ml of saline) at a dose of 30 mg/kg/day was administered i.p. for 14 days. In the AL + NC group, 150 mg/kg NAC was administered 1 h after daily 30 mg/kg AL i.p. administration for 14 days. NAC (Ampoule containing Asist® 300 mg/3 ml (10%) solution) was purchased from Hüsnu Arsan Farma Turkey. The doses of NAC [9] and AL [16] used in this study were referenced from previous studies. Upon completion of all procedures (15th day), the experiment was finalized. The experimental rats were sacrificed under anesthesia (ketamine (75 mg/kg) + xylazine (10 mg/kg) administered i.p.).

Table 1 Essential nutrient content in standard rat feed

PROTEIN	23.5%
RAW cELLULOSE	6.12%
RAW aSH	5.26%
RAW oIL	3.26%
LYSINE	1.26%
PHOSPHORUS	0.76%
CALCIUM	0.58%
METHIONINE	0.43%
SODIUM	0.05%

Intracardiac blood was drawn for use in biochemical analysis. Blood serum was preserved at $-80\text{ }^\circ\text{C}$ until the analysis of blood urea nitrogen (BUN) and creatinine. Kidney tissues were quickly removed. While some of the kidney tissues were used for histopathological and immunohistochemical evaluations, some were stored at $-80\text{ }^\circ\text{C}$ for biochemical evaluations. For biochemical evaluations, kidney tissues were homogenized in 10% phosphate buffer solution (PBS). Homogenized samples were centrifuged at 5000 rpm at $+4\text{ }^\circ\text{C}$ for 20 min. The supernatants were then preserved at $-80\text{ }^\circ\text{C}$ until the analysis of SPX levels, total antioxidant status (TAS), and total oxidant status (TOS).

Histopathological Evaluation

Kidney tissues were rapidly removed and put in the 10% formaline solution for histopathological evaluations. After tissue fixation, the kidney tissues were run through the routine histological investigation steps and were buried in paraffin blocks. A 5- μm -thick cross-sections were taken from the paraffin blocks. After removing the paraffin of the sections with xylene, they were passed through serially diluted alcohol solutions. For the general histopathological evaluations, hematoxylin–eosin (HE) staining procedures were applied. The prepares that were applied with the histological staining methods were studied under optical microscope (DM2500 LED, Leica, Germany) and photographed (MC170 HD, Leica, Germany).

Immunohistochemical Examination

In order to determine the Bcl-2, Bcl-2 associated x (Bax), Casp3 and SPX immunoreactivities in the kidney tissues, avidin–biotin–peroxidase complex method was used. The 5- μm -thick cross-sections taken from the cooled paraffin blocks were placed on polylysine coated glass slides. Following the deparaffinization and transparentization with xylol, the tissues were passed through serially diluted alcohol solutions and were boiled in microwave oven (750 W) for 12 min while in citrate buffer solution ($\text{pH} = 6.0$). After coiling for approximately 20 min at room temperature, the tissues were washed with PBS (Phosphate Buffered Saline, P4417, Sigma-Aldrich, ABD) for 3×5 min and were incubated in hydrogen peroxide block (H_2O_2 block) solution for 5 min in order to inhibit the endogenous peroxidase activity (Hydrogen Peroxide Block, TA-125-HP, Lab Vision Corporation, USA). In order to prevent the base staining on the tissues that were washed with PBS for 3×5 min, Ultra V Block (TA-125-UB, Lab Vision Corporation, USA) solution was applied for 5 min, which

was followed by dripping the primer antibodies. Tissues were then incubated with BcL-2 primer antibody (Sun-Red-201r.5304, China), Bax primer antibody (Santa Cruz Biotechnology, sc-7480, California, USA), Casp3 primer antibody (bs-0081R, Bioss Inc, Beijing, China), and SPX primer antibody (A04088-1, Boster Biological Technology, Pleasanton, CA, USA) for 60 min in the lab oven at 37 °C temperature. The preparates that were washed with PBS were incubated with the secondary antibody (TP-060-BN, Thermo Scientific, England) for 30 min at room temperature in humid and dark ambient. After incubation, the tissues washed with PBS were dripped with Horse Radish Peroxidase (HRP) enzyme (TS-060-HR, Thermo Scientific, England) and were incubated for 30 min at room temperature in humid ambient. 3-amino-9-ethyl carbazole (AEC) substrate solution (TA-060-HA, Thermo Scientific, England) was dripped on the tissues. After receiving the image signal from the optical microscope, the reaction was terminated simultaneously in all tissues by distilled water. Reverse staining was performed with Harris hematoxylin. The preparates, which were first washed with water, were then closed by a water-based cover solution (TA-125-UG, Lab Vision Corporation, USA). Finalized preparates were studied under an optical microscope (DM2500 LED, Leica, Germany) and were photographed (MC170 HD, Leica, Germany). Immunohistochemical evaluation was made according to the spread of the immunoreactivity (0.1: < %25, 0.4: %26–50, 0.6: %51–75, 0.9: %76–100) and magnitude (0: none, 0.5: very little, 1: little, 2: medium, 3: high). Histoscoring table was created based on the product of these two results.

Terminal Deoxynucleotidyl Transferase dUTP Nick-End Labeling (TUNEL) Analysis

A 4- μ m-thick sections from kidney tissue paraffin blocks were taken to polylysis coated slides. TUNEL test (TUNEL Assay Kit – HRP – DAB, ab206386, Abcam) was studied according to the manufacturer's instructions and apoptotic cell level was determined. As a result of TUNEL painting, core cells painted green with methyl green were considered normal and cells with brown cores were considered apoptotic. The percentages of TUNEL-positive cells were quantified by counting 500 cells from ten random microscopic areas and an Apoptotic Index (AI) was calculated [17].

$$\text{AI} = \frac{(\text{total number of cells counted} - \text{total number of living cells})}{\text{total number of cells counted}} \times 100$$

Biochemical Analyses

BUN and Creatinine Levels in Serum

BUN and creatinine levels in blood serum were measured using a Siemens ADVIA 2400 automatic biochemical analyzer and kit.

Determination of SPX, TAS and TOS Levels

Enzyme-linked immunosorbent assay (ELISA) method was performed to determine the total oxidant/antioxidant (TAS and TOS) and SPX levels in kidney tissue samples. SPX (Lot:2,022,105, Shanghai Coon Biotech, Shanghai, China), TAS (AD3283Ra, AndyGene, TX75081, USA) and TOS (AD3282Ra, AndyGene TX75081, USA) ELISA kits that allow quantitative measurement in rat tissue samples were purchased. Analyses were performed according to the protocols of the kits. Test results were presented as pg/ml, U/ml, and pg/ml, respectively. The SPX test range was 79–5000 pg/ml and its sensitivity was 55.36 pg/ml; the TAS test range was 0.2–8 U/ml and its sensitivity was 0.1 U/ml; the TOS test range was 3.75–120 pg/ml and its sensitivity was 0.7 pg/ml.

Statistical Analysis

Statistical package for SPSS 22.0 package program was used in the analysis of the data obtained within the scope of the research. The data were presented as standard error (SE) ($n = 7$) with an average \pm . The fitness of the data with normal distribution was checked by Shapiro–Wilk test. One-way ANOVA and post hoc Tukey test were used in the statistical analysis of the results. The value of $p < 0.05$ was considered statistically significant. The graphics were drawn using the software GraphPad Prism 9.3.1.

G Power Analysis

The analysis was made in G*Power version 3.1 (University Kiel, Germany). The sample size in each group was determined as 7 rats by strength analysis with a type 1 error (α) of 0.05 and a power of 0.90 [18].

Results

Effect of NAC Treatment on Rat Kidney Tissue Histopathology After AL Exposure

Normal histological kidney tissue was observed in the control group (Fig. 1a1 and a2). The NC group had normal histological glomerular and tubular structures similar to the

control group (Fig. 1b1 and b2). In the AL group kidney tissues, vascular congestion, hemorrhagic areas, inflammatory cells, and tubular degeneration were observed (Fig. 1c1 and c2). Moreover, glomerular structures were mostly hypertrophic and Bowman's space was narrowed. In the AL + NC group, in which NAC was applied after AL exposure, AL-induced histopathological changes were less/mitigated (Fig. 1d1 and d2).

Effect of AL Exposure and Subsequent NAC Treatment on Bcl-2, Bax, Casp3 and SPX Immunoreactivities in Rat Kidney Tissue

Bcl-2 immunoreactivity in kidney tissue was similar in the control and NC groups ($p > 0.05$) (Fig. 2A(a, b)). In the AL group, AL exposure relatively decreased the Bcl-2 immunoreactivity in kidney tissue compared to the control group, but this decrease was not statistically significant ($p = 0.176$) (Fig. 2A(c)). NAC administration relatively increased Bcl-2 immunoreactivity in the AL + NC group compared to the AL group ($p = 0.530$) (Fig. 2A(d), Table 2).

Bax immunoreactivity was similar in kidney tissue in the control and NC groups ($p > 0.05$) (Fig. 2B(a, b)). AL exposure significantly increased Bax immunoreactivity compared to control group ($p < 0.001$) (Fig. 2B(c)). Bax immunoreactivity relatively decreased in the AL + NC group compared to the AL group, but this decrease was not statistically significant ($p = 0.207$) (Fig. 2B(d), Table 2).

Similarly, Casp3 immunoreactivity in kidney tissue was similar in the control and NC groups ($p > 0.05$) (Fig. 2C(a, b)). Casp3 immunoreactivity significantly increased in the AL group compared to the control group ($p < 0.001$) (Fig. 2C(c)). In the AL + NC group, Casp3

immunoreactivity significantly decreased compared to the AL group ($p = 0.046$) (Fig. 2C(d), Table 2).

SPX immunoreactivity in kidney tissue was similar in the control and NC groups ($p > 0.05$) (Fig. 2E(a, b)). AL exposure significantly increased SPX immunoreactivity compared to the control group ($p = 0.001$) (Fig. 2E(c)). In the AL + NC group, SPX immunoreactivity relatively decreased compared to the AL group, but this decrease was not statistically significant ($p = 0.144$, Table 2).

Effect of AL and/or NAC Application on AI in the Kidney

Kidney tissues subjected to the TUNEL staining procedure were examined under a light microscope. Apoptotic cells were observed in the glomerular and tubular areas (Fig. 2D). AI was statistically significantly higher in the AL group compared to the control group ($p < 0.001$, Table 2). Apoptotic cells and AI significantly decreased in the AL + NC group compared to the AL group (Fig. 2D (d), $p < 0.001$). NAC treatment was found to ensure protection against AL-induced increased apoptotic cells.

Effect of AL and/or NAC Application on Biochemical Parameters and SPX Level in Kidney Tissue

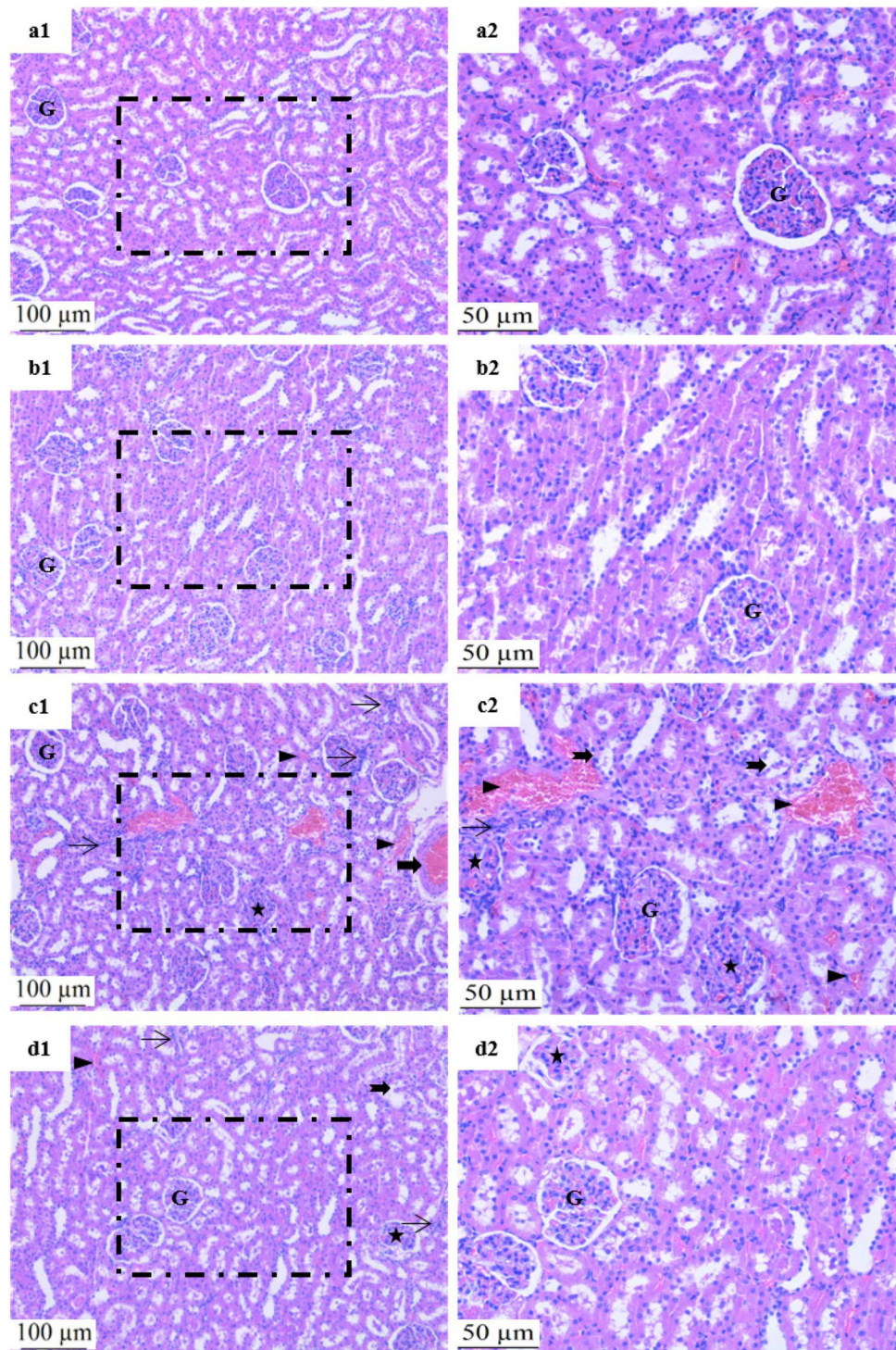
Serum BUN and creatinine levels were similar in the control and NC groups (Fig. 3, $p > 0.05$). BUN and creatinine levels significantly increased in the AL group compared to the control group (Fig. 3, *, $p < 0.001$). However, there was a statistically significant decrease in BUN and creatinine levels in the AL + NC group compared to the AL group (Fig. 3; #, $p < 0.001$).

Table 2 Effect of AL and/or NAC administration on Bcl-2, Bax, Casp3, SPX immunoreactivities and AI in kidney tissue

	Control	NC	AL	AL + NC	P
BCL-2	1.22 ± 0.17	1.17 ± 0.18	0.74 ± 0.12	1.05 ± 0.16	0.177
BAX	0.16 ± 0.04	0.23 ± 0.07 ^b	1.61 ± 0.23 ^a	1.17 ± 0.18 ^a	<0.001
CASP3	0.20 ± 0.05	0.17 ± 0.04 ^b	1.05 ± 0.16 ^a	0.65 ± 0.10 ^{ab}	<0.001
AI	2.35 ± 0.07	2.23 ± 0.05 ^b	8.09 ± 0.10 ^a	5.66 ± 0.10 ^{ab}	<0.001
SPX	0.71 ± 0.09	0.77 ± 0.12 ^b	1.67 ± 0.20 ^a	1.17 ± 0.18	0.001

Values are presented as mean ± standard error. Bcl-2, Bax, Casp3, SPX immunoreactivities, and AI in kidney tissue were similar in the control and NC groups ($p > 0.05$). Bcl-2 immunoreactivity was relatively decreased in the AL group compared to the control group ($p = 0.176$). Bcl-2 immunoreactivity was relatively increased in the AL + NC group compared to the AL group ($p = 0.530$). Bax immunoreactivity was significantly increased in the AL group compared to the control group ($p < 0.001$). Bax immunoreactivity was relatively decreased in the AL + NC group compared to the AL group ($p = 0.207$). Casp3 immunoreactivity was significantly increased in the AL group compared to the control group ($p < 0.001$). In the AL + NC group, Casp3 immunoreactivity was significantly reduced compared to the AL group ($p = 0.046$). AI was statistically significantly higher in the AL group compared to the control group ($p < 0.001$). AI significantly decreased in the AL + NC group compared to the AL group ($p < 0.001$). SPX immunoreactivity was significantly increased in the AL group compared to the control group ($p = 0.001$). SPX immunoreactivity was relatively decreased in the AL + NC group compared to the AL group ($p = 0.144$). ^aCompared with the control group, ^bcompared with the AL group ($p < 0.05$). AI apoptotic index, Bax Bcl-2 associated x, Casp3 caspase 3, SPX spexin; Groups: AL aluminum, NC N-acetylcysteine

Fig. 1 Effect of AL exposure and subsequent NAC treatment on kidney tissue histopathology. Photomicrographs showing the normal histological appearance of kidney tissue in groups Control (**a1**, **a2**) and NC (**b1**, **b2**). In the AL group; areas of inflammation (thin arrow), hemorrhagic areas (triangle), glomerulus degeneration (asterix), tubular degeneration (notched arrow) and vascular congestion (thick arrow) was observed (**c1**, **c2**). In the AL + NC group, it was determined that the histopathological changes in the AL group were alleviated/decreased (**d1**, **d2**). Hematoxylin eosin, scale bar: 100 μm , $\times 200$ (**a1**, **b1**, **c1**, **d1**); 50 μm , $\times 400$ (**a2**, **b2**, **c2**, **d2**). AL, aluminum; G, Glomerulus; NAC, N-acetylcysteine; groups: AL, aluminum; NC, N-acetylcysteine



SPX levels in kidney tissue homogenates were similar in the Control and NC groups (Fig. 3, $p > 0.05$). SPX levels significantly increased in the AL group compared to the control group (Fig. 3, *, $p < 0.001$). SPX levels decreased in the AL + NC group compared to the AL group (Fig. 3; #, $p < 0.001$).

Effect of AL on Oxidative Stress Parameters in Kidney Tissue

TAS and TOS levels in kidney tissue were similar in the control and NC groups (Fig. 4, $p > 0.05$). There was a decrease in kidney TAS in the AL group compared to the control

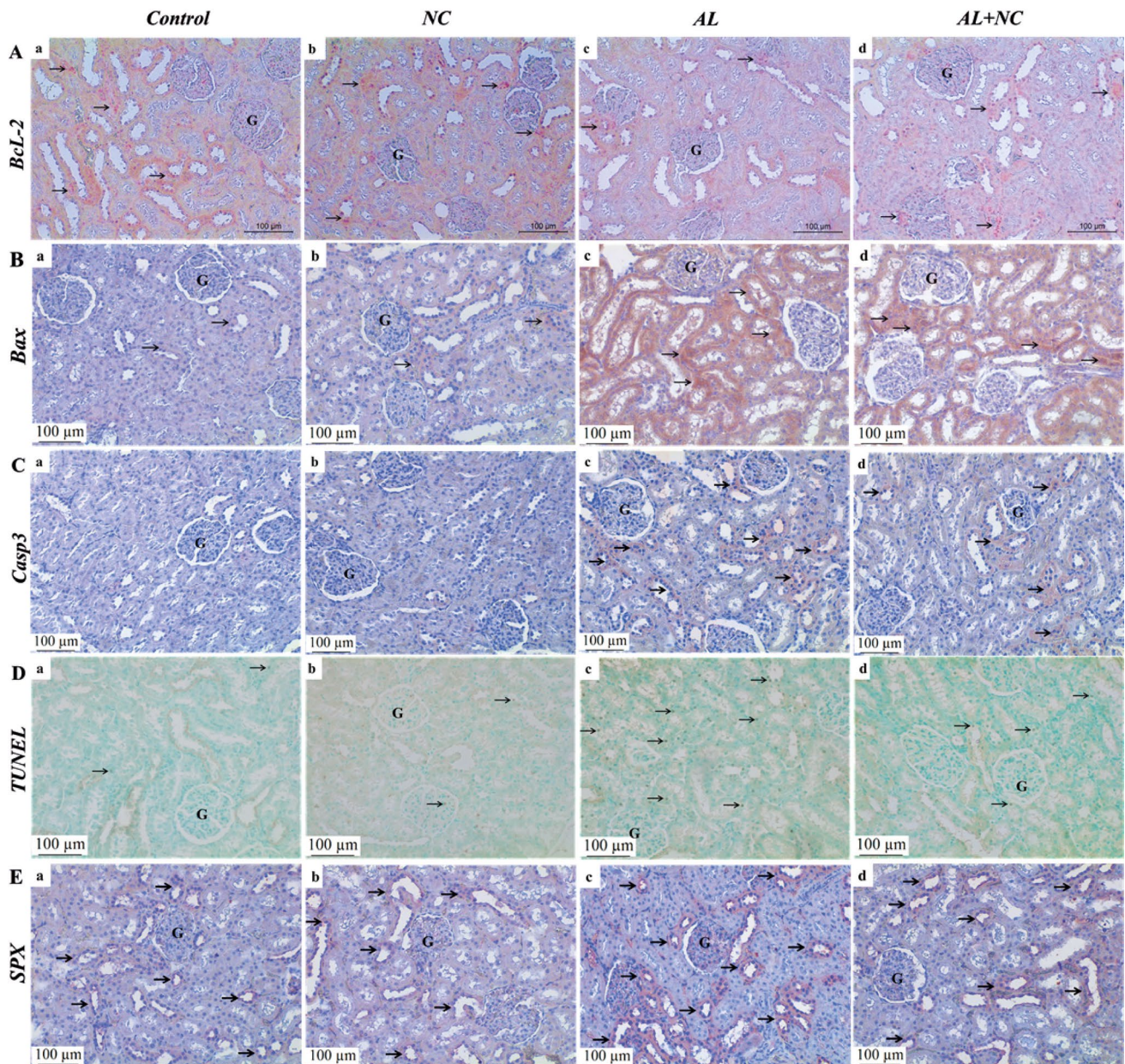


Fig. 2 Effects of AL and/or NAC administration on kidney tissue Bcl-2, Bax, Casp3, SPX immunoreactivities, and TUNEL staining photomicrographs. It was observed that kidney tissues in control and NC groups had similar Bcl-2, Bax, Casp3, SPX immunoreactivities ($p > 0.05$) (a, b). It was determined that Bcl-2 immunoreactivity was relatively decreased in AL group (A; c) compared to Control group, but this decrease was not statistically significant ($p > 0.05$). In the AL+NC group, (A; d) Bcl-2 immunoreactivity was relatively increased compared to the AL group, but this increase was not statistically significant ($p > 0.05$). It was determined that Bax immunoreactivity was significantly increased in AL group (B; c) compared to the control group ($p < 0.05$). In the AL+NC group (B; d), Bax immunoreactivity was relatively decreased compared to the AL group, but this was not statistically significant ($p > 0.05$). It was determined that Casp3 immunoreactivity was significantly increased in AL group (C; c) compared to Control group ($p < 0.05$). In the AL+NC group (C; d), Casp3 immunoreactivity was statistically significantly

decreased compared to the AL group ($p < 0.05$). It was determined that SPX immunoreactivity was significantly increased in AL group (E; c) compared to control group ($p < 0.05$). In the AL+NC group (E; d), SPX immunoreactivity was relatively decreased compared to the AL group ($p > 0.05$). A Bcl-2 immunohistochemical images, B Bax immunohistochemical images, C Casp3 immunohistochemical images, E SPX immunohistochemical images. D TUNEL staining photomicrographs, arrows indicates TUNEL positive cells labeled as brown nuclei. TUNEL positive cells were at similar rates in the control and NC groups (a, b, $p > 0.05$). TUNEL positive cells were significantly increased in AL group compared to control and NC groups (D; c, $p < 0.05$). Compared with the AL group, TUNEL positive cells were significantly reduced in the AL+NC group (D; d, $p < 0.05$). All slides were counterstained with methyl green. Scale bar: 100 μm , $\times 200$. G, glomerulus; Arrow, immunoreactivity; Bax, Bcl-2 associated x; Casp3, caspase 3; SPX, spexin; Groups: AL, aluminum; NC, N-acetylcysteine

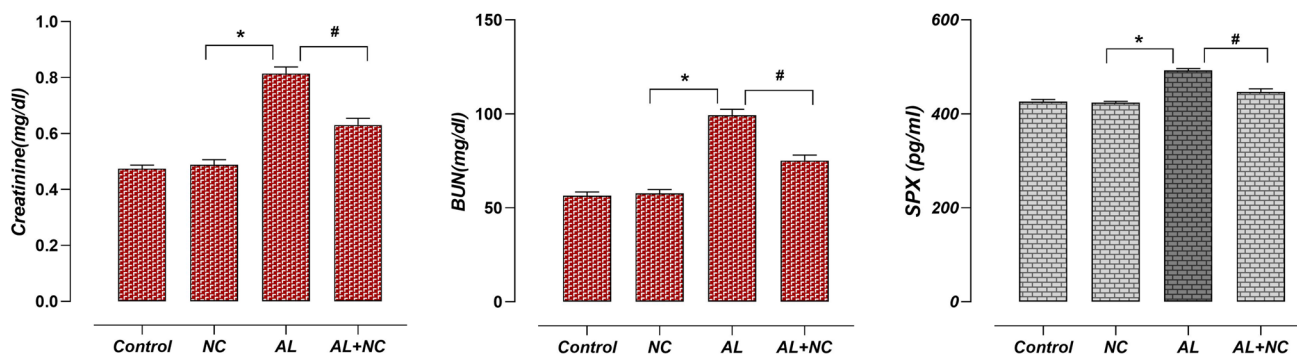


Fig. 3 Effects of AL and/or NAC administration on serum creatinine, BUN, and kidney tissue SPX levels. The creatinine, BUN, and SPX levels were similar in the control and NC groups ($p > 0.05$). Serum creatinine and BUN levels increased significantly in AL group compared to control and NC groups (*, $p < 0.05$). In the AL+NC group, it was statistically significantly decreased compared to the AL group (#, $p < 0.05$). SPX level in kidney tissue increased significantly in AL

group compared to control and NC groups (*, $p < 0.05$). SPX level decreased significantly in AL+NC group compared to AL group (#, $p < 0.05$). Values are presented as mean \pm standard error. *: $p < 0.05$ compared with control and NC groups, #: $p < 0.05$ compared with group AL. BUN, blood urea nitrogen; SPX, spexin; Groups: AL, aluminum; NC, N-acetylcysteine

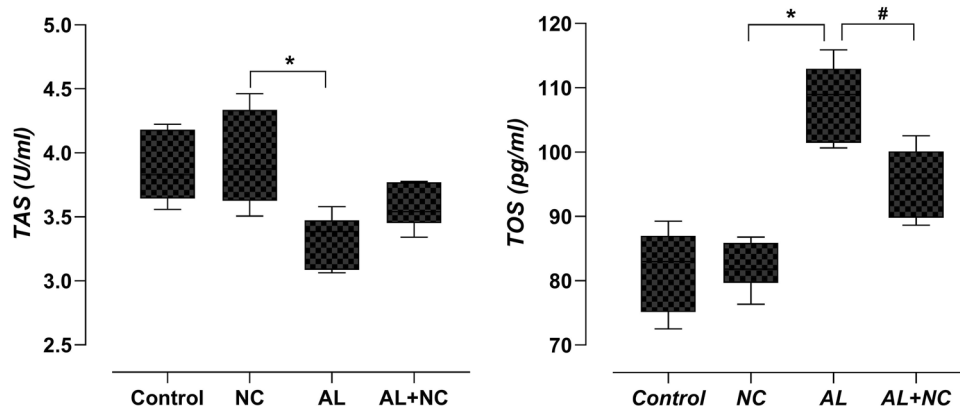


Fig. 4 Effects of AL and/or NAC administration on TAS and TOS levels in kidney tissue. TAS and TOS levels were similar in control and NC groups ($p > 0.05$). TAS levels decreased significantly in AL group compared to Control and NC groups, while TOS levels increased (*, $p < 0.05$). TAS levels increased relatively in the AL+NC group compared to the AL group, while TOS lev-

els decreased significantly (#, $p < 0.05$). Values are presented as mean \pm standard error. *: $p < 0.05$ compared to control and NC groups, #: $p < 0.05$ compared to group AL. TAS, total antioxidant status; TOS, total oxidant status; Groups: AL, aluminum, NC, N-acetylcysteine

group (Fig. 4, *, $p = 0.002$). However, kidney TOS levels significantly increased in the AL group compared to the control group (Fig. 4, *, $p < 0.001$). Furthermore, TAS values relatively increased ($p = 0.202$), whereas TOS levels significantly decreased in the AL+NC group compared to the AL group (Fig. 4; #, $p < 0.001$).

Discussion

Today, AL is well-known as a nephrotoxic agent. Its toxic effects arise due to the high risk of daily exposure [19]. Studies reported that markers such as creatinine and urea that increase with kidney tissue damage increase due to AL

exposure [4, 7]. Consistent with these data, in the current study, it was found that AL exposure significantly increased BUN and creatinine levels (Fig. 3). On the other hand, studies reported that AL causes renal oxidative damage by causing a decrease in antioxidant parameters and an increase in oxidant parameters [4–6]. Likewise, this study showed that AL can cause oxidative stress by decreasing the TAS level and increasing the TOS level in kidney tissue (Fig. 4).

It was previously stated that the pathological basis of AL toxicity is oxidative stress and apoptosis [20]. Expression of the anti-apoptotic Bcl-2 protein, which plays an important role in the regulation of apoptotic cell death, significantly decreased in rats exposed to AL [4]. In the current study, it was observed that the level of Bcl-2 protein relatively

decreased in the AL group compared to the control group. These results support that AL may cause apoptosis in kidney tissue by decreasing Bcl-2 expression [21]. In addition, prolongation of the activation of c-Jun N-terminal kinase (JNK) due to increased ROS promotes regulation of Bcl-2 inactivation and translocation of Bax and caspase-8 to mitochondria. This is important for the proapoptotic function of JNK. Studies suggested that AL causes apoptotic damage by increasing hepatic mitogen-activated protein kinase (MAPK) and the expression of JNK protein [22]. Consistent with these data, the results obtained in the present study demonstrated that AL exposure causes apoptotic damage by decreasing Bcl-2 immunoreactivity and increasing Bax and Casp3 immunoreactivities in kidney tissue ($p < 0.05$). These results were also further confirmed with the TUNEL method (Table 2).

In a study, it was shown that NAC alleviates AL-induced damages by possibly removing free radicals, binding AL, stimulating its excretion, reducing its bioavailability, strengthening endogenous antioxidant defense systems, and stabilizing the cell membrane when administered at 150 mg/kg simultaneously or after AL exposure [23]. The current study showed that NAC treatment (150 mg/kg) may have a protective effect on kidney tissue by regulating histopathological changes caused by AL, increased renal biochemical markers, oxidative stress parameters, and apoptotic protein levels (Figs. 1, 2, 3, and 4, Table 2).

SPX was reported to be a potential regulatory factor in obesity and energy metabolism [24]. Pioneering studies reported that SPX immunoreactivity is localized in kidney tissue, primarily epithelial cells in Henle loop and distal tubules, and that expression is not observed in the proximal tubules [25]. In the current study, it was observed that SPX showed immunoreactivity, especially in epithelial cells of the distal tubules (Fig. 2). Additionally, it was reported that SPX administration improves body weight and composition, glucose metabolism, insulin sensitivity, liver function, and hormonal profiles in type 2 diabetes and diet-induced obesity in rodents [26]. A study reported that SPX administration alleviated dyslipidemia and insulin resistance in rats fed a high-fructose diet [27]. It is known that SPX shows inhibitory effects on reproduction and nutrition through galanin receptor 2 (GALR2) and galanin receptor 3 (GALR3) [28]. GALR3 signaling was reported to alleviate cellular stress and apoptosis in subventricular neural stem cells exposed to high glucose and palmitate [29]. In addition, a study reported that SPX treatment regulates impaired glucose and lipid metabolism and inhibits hypoxia-induced mitochondrial dysfunction and oxidative stress through GAL2R activation in cardiomyocytes [30]. A recent study reported that high-fat fructose diet caused an increase in histopathological and biochemical parameters in rat kidney tissues, resulting in renal dysfunction. In the same study, it was shown that

SPX treatment significantly reduced histopathological and biochemical parameters. In addition, it has been reported that SPX has an anti-oxidative effect by returning GSH to normal levels and an anti-apoptotic effect by suppressing the apoptotic marker Casp3 [31]. The suppression of these effects of SPX in the group receiving the GALR-2 antagonist M871 was interpreted as that SPX ameliorated these morphological changes through GALR-2 [30, 31].

In this current study, it was observed that SPX levels increased in AL-induced kidney tissue damage (Table 2, Fig. 3). Recent studies have revealed that experimental induction of dietary saturated fatty acid and hyperglycemia directly affects SPX expression and secretion [28, 32, 33]. After short-term administration of insulin or glucose, SPX release and SPX-immunoreaction are increased in cultured cells and isolated islets [34, 35]. Also in vitro, SPX mRNA levels have been reported to increase in hypothalamic neurons after acute treatments with saturated fatty acid palmitate [28, 32]. Additionally, plasma or hypothalamic SPX levels were increased after treatment with glucose or insulin in goldfish [35]. These results suggest that SPX may be induced by an acute metabolic disorder, providing a protective mechanism against metabolic dysfunction [36].

In the light of this information, in the current study, it was observed that SPX secretion and immunoreactivity in kidney tissues increased under reduced physiological conditions due to acute AL nephrotoxicity. In addition, we believe that it may be effective in increasing the level of SPX in AL-induced oxidative stress in kidney tissue. Because while SPX levels increased in the AL group, they decreased significantly in parallel with the regulation of oxidative stress parameters in the AL + NC group. These results show that SPX is sensitive to oxidative stress.

Conclusion

In this study, we explained the effect of NAC on AL-induced kidney tissue damage by evaluating histopathological changes, biochemical markers, apoptotic protein levels, and oxidative stress parameters. As a result, we showed that AL-induced histopathological changes, oxidative stress, and apoptosis were increased in kidney tissue. We also found that SPX, which plays a role in energy metabolism, increases in AL-induced kidney damage. We explained that NAC has a protective effect against kidney damage by showing its antioxidant and antiapoptotic properties in kidney tissue. However, we observed that NAC attenuated the AL-induced increased SPX level by attenuating oxidative stress. We think that our study will shed light on future studies and will play an important role in determining the role of SPX in kidney tissue damage.

Data Availability The datasets generated during and/or analysed during the current study are available from the corresponding author on reasonable request.

Declarations

Competing Interests The authors declare no competing interests.

References

- Klotz K, Weistenhöfer W, Neff F, Hartwig A, van Thriel C, Drexler H (2017) The health effects of aluminum exposure. *Dtsch Arztebl Int* 114(39):653. <https://doi.org/10.3238/arztebl.2017.0653>
- Zhu Y, Hu C, Zheng P, Miao L, Yan X, Li H et al (2016) Ginsenoside Rb1 alleviates aluminum chloride-induced rat osteoblasts dysfunction. *Toxicology* 368:183–188. <https://doi.org/10.1016/j.tox.2016.07.014>
- Balagoon MJ (2019) Assessment of the protective effect of lepidium sativum against aluminum-induced liver and kidney effects in albino rat. *Biomed Res Int* 2:1–9. <https://doi.org/10.1155/2019/4516730>
- Othman MS, et al (2020) The protective effects of melatonin on aluminum-induced hepatotoxicity and nephrotoxicity in rats. *Oxidative Medicine and Cellular Longevity*, Article ID 7375136, 12. <https://doi.org/10.1155/2020/7375136>
- Yousef MI et al (2019) Hepato-renal toxicity of oral sub-chronic exposure to aluminum oxide and/or zinc oxide nanoparticles in rats. *Toxicol Rep* 19(6):336–346. <https://doi.org/10.1016/j.toxrep.2019.04.003>
- Zahedi-Amiri Z, Taravati A, Hejazian LB (2019) Protective effect of rosa damascena against aluminum chloride-induced oxidative stress. *Biol Trace Elem Res* 187(1):120–127. <https://doi.org/10.1007/s12011-018-1348-4>
- Al-Kahtani M, Morsy K (2019) Ameliorative effect of selenium nanoparticles against aluminum chloride-induced hepatorenal toxicity in rats. *Environ Sci Pollut Res* 26:32189–33219. <https://doi.org/10.1007/s11356-019-06417-y>
- Tras B et al (2021) Treatment and protective effects of metalloproteinase inhibitors alone and in combination with N-acetyl cysteine plus vitamin E in rats exposed to aflatoxin B1. *Toxicol* 30(194):79–85. <https://doi.org/10.1016/j.toxicol.2021.02.012>
- Elsayed A, Elkomy A, Elkammar R et al (2021) Synergistic protective effects of lycopene and N-acetylcysteine against cisplatin-induced hepatorenal toxicity in rats. *Sci Rep* 11(1):13979. <https://doi.org/10.1038/s41598-021-93196-7>
- Owumi SE et al (2021) N-acetyl cysteine co-treatment abates perfluorooctanoic acid-induced reproductive toxicity in male rats. *Andrologia* 53:e14037. <https://doi.org/10.1111/and.14037>
- Pruszyńska-Oszmalek E et al (2020) Short-term administration of spexin in rats reduces obesity by affecting lipolysis and lipogenesis: an in vivo and in vitro study. *Gen Comp Endocrinol* 299:113615. <https://doi.org/10.1016/j.ygcen.2020.113615>
- Chen T, Wang F et al (2019) Circulating spexin decreased and negatively correlated with systemic insulin sensitivity and pancreatic β cell function in obese children. *Ann Nutr Metab* 74(2):125–131. <https://doi.org/10.1159/000496459>
- Gu L et al (2019) Spexin alleviates insulin resistance and inhibits hepatic gluconeogenesis via the foxo1/pgc-1 α pathway in high-fat-diet-induced rats and insulin resistant cells. *Int J Biol Sci* 15(13):2815–2829. <https://doi.org/10.7150/ijbs.31781>
- Karaca A et al (2019) Decreased spexin levels in patients with type 1 and type 2 diabetes. *Med Princ Pract* 27(6):549–554. <https://doi.org/10.1159/000493482>
- Behrooz M, Vaghef-Mehrabany E, Ostadrahimi A (2020) Different spexin level in obese vs normal weight children and its relationship with obesity related risk factors. *Nutr Metab Cardiovasc Dis* 30(4):674–682. <https://doi.org/10.1016/j.numecd.2019.11.008>
- Yang X, Yuan Y, Niu Q (2016) Effects of aluminium chloride on the methylation of app in hippocampal of rats. *J Hyg Res* 45(3):345–349 (PMID: 27459792)
- Gul HF et al (2021) The combined effect of pomegranate extract and tangeretin on the DMBA-induced breast cancer model. *J Nutr Biochem* 89:108566. <https://doi.org/10.1016/j.jnutbio.2020.108566>
- Faul F et al (2009) Statistical power analyses using G*Power 3.1: tests for correlation and regression analyses. *Behav Res Methods* 41:1149–1160. <https://doi.org/10.3758/BRM.41.4.1149>
- Emara NA, Mahmoud MF, El Fayoumi HM et al (2021) The renoprotective effect of glycyrrhizic acid in insulin-resistant rats exposed to aluminum involves the inhibition of TLR4/NF- κ B signaling pathway. *Naunyn Schmiedebergs Arch Pharmacol* 394:863–872. <https://doi.org/10.1007/s00210-020-02012-y>
- Xu F, Liu Y, Zhao H et al (2017) Aluminum chloride caused liver dysfunction and mitochondrial energy metabolism disorder in rat. *J Inorg Biochem* 174:55–62. <https://doi.org/10.1016/j.jinorgbio.2017.04.016>
- Li M et al (2016) AIC13 induces lymphocyte apoptosis in rats through the mitochondria-caspase dependent pathway. *Environ Toxicol* 31(4):385–394. <https://doi.org/10.1002/tox.22051>
- Hassan SA, Kadry MO (2021) Neurodegenerative and hepatorenal disorders induced via aluminum chloride in murine system: impact of β -secretase, MAPK, and KIM. *Biol Trace Elem Res* 199(1):227–236. <https://doi.org/10.1007/s12011-020-02132-9>
- Nour-Eldein NH et al (2018) mitigation of acute aluminum toxicity by sodium selenite and n-acetylcysteine in adult male rats. *Biol Trace Elem Res* 183(1):128–137. <https://doi.org/10.1007/s12011-017-1126-8>
- Wang X, Wang S, Feng W, Wang R, Zhang H, Yang X et al (2016) Research progress of spexin in energy metabolism in Chemistry of Life 36:852–855. <https://doi.org/10.3389/fphar.2019.00457>
- Porzionato A et al (2010) Spexin expression in normal rat tissues. *J Histochem Cytochem* 58(9):825–837. <https://doi.org/10.1369/jhc.2010.956300>
- Kołodziejwski PA et al (2021) The role of peptide hormones discovered in the 21st century in the regulation of adipose tissue functions. *Genes (Basel)* 12(5):756. <https://doi.org/10.3390/genes12050756>
- Said MA et al (2021) Spexin alleviates hypertension, hyperuricaemia, dyslipidemia and insulin resistance in high fructose diet induced metabolic syndrome in rats via enhancing PPAR- γ and AMPK and inhibiting IL-6 and TNF- α . *Arch Physiol Biochem* 15:1–6. <https://doi.org/10.1080/13813455.2021.1899242>
- Wang L et al (2020) Palmitate differentially regulates Spexin, and its receptors Galr2 and Galr3, in GnRH neurons through mechanisms involving PKC, MAPKs, and TLR4. *Mol Cell Endocrinol* 1(518):110991. <https://doi.org/10.1016/j.mce.2020.110991>
- Mansouri S et al (2013) GalR3 activation promotes adult neural stem cell survival in response to a diabetic milieu. *J Neurochem* 127:209–220. <https://doi.org/10.1111/jnc.12396>
- Liu Y, Sun L, Zheng L, Su M, Liu H, Wei Y, Li D, Wang Y, Dai C, Gong Y, Zhao C, Li Y (2020) Spexin protects cardiomyocytes from hypoxia-induced metabolic and mitochondrial dysfunction. *Naunyn Schmiedebergs Arch Pharmacol* 393:25–33. <https://doi.org/10.1007/s00210-019-01708-0>
- El-Saka MH, Abo El Gheit RE, El Saadany A, Alghazaly GM, Marea KE, Madi NM (2021) Effect of spexin on renal dysfunction

- in experimentally obese rats: potential mitigating mechanisms via galanin receptor-2. *Arch Physiol Biochem*. <https://doi.org/10.1080/13813455.2021.1887265>
32. Tran A, Loganathan N, McIlwraith EK et al (2020) Palmitate and nitric oxide regulate the expression of spexin and galanin receptors 2 and 3 in hypothalamic neurons. *Neuroscience* 447:41–52. <https://doi.org/10.1016/j.neuroscience.2019.10.028>
33. Behrooz M, Vaghef-Mehrabany E, Moludi J, Ostadrahimi A (2021) Are spexin levels associated with metabolic syndrome, dietary intakes and body composition in children? *Diabetes Res Clin Pract* 172:108634. <https://doi.org/10.1016/j.diabres.2020.108634>
34. Sassek M, Kołodziejwski PA, Szczepankiewicz D, Pruszyńska-Oszmalko E (2019) Spexin in the physiology of pancreatic islets—mutual interactions with insulin. *Endocrine* 63(3):513–519. <https://doi.org/10.1007/s12020-018-1766-2>
35. Ma A, He M, Bai J, Wong MK, Ko WK, Wong AO (2017) Dual role of insulin in spexin regulation: functional link between food intake and spexin expression in a fish model. *Endocrinology* 158(3):560–577. <https://doi.org/10.1210/en.2016-1534>
36. Fang P, Ge R, She Y, Zhao J, Yan J, Yu X et al (2022) Adipose tissue spexin in physical exercise and age-associated diseases. *Ageing Res Rev* 73:101509. <https://doi.org/10.1016/j.arr.2021.101509>

Publisher's Note Springer Nature remains neutral with regard to jurisdictional claims in published maps and institutional affiliations.